FUBP3 regulates expression and alternative splicing of genes associated with cell proliferation and apoptosis in cancer cells

LINGYU KONG[1], CHAOXU FU[2], XUESONG LI[3], MINGXIN CHEN[4], XINQI LIU[1], MIN ZHOU[5], TONGSHU WANG[6] and HONGXIN PIAO[7]

[1]Department of Internal Medicine, Yanbian University School of Medicine, Yanji, Yanbian Korean Autonomous Prefecture, Jilin 133002, P.R. China; [2]Molecular Diagnostics Laboratory, Precision Molecular Medicine Center, Jilin Province People's Hospital, Changchun, Jilin 130021, P.R. China; [3]Emergency Department, Yanbian University Affiliated Hospital, Yanji, Yanbian Korean Autonomous Prefecture, Jilin 133099, P.R. China; [4]Emergency and Outpatient Department, China-Japan Union Hospital of Jilin University, Changchun, Jilin 130033, P.R. China; [5]Clinical Research Laboratory, Clinical Trial Research Center, Zibo Central Hospital, Zibo, Shandong 250036, P.R. China; [6]Department of Internal Medicine, Panshi Hospital, Panshi, Jilin 132300, P.R. China; [7]Department of Infectious Diseases, Affiliated Hospital of Yanbian University, Yanji, Yanbian Korean Autonomous Prefecture, Jilin 133099, P.R. China

Received November 26, 2025; Accepted June 12, 2026

DOI: 10.3892/ol.2026.15751

Abstract. Far upstream element binding protein (FUBP)3, a member of the FUBP family of proteins, is a DNA-binding transcription activator and an RNA-binding protein. FUBP3 is deregulated in various types of human cancer and promotes cell proliferation. However, the underlying molecular mechanism of FUBP3 in cancer is still unclear. Therefore, the present study investigated the cell biology, gene expression profile and alternative splicing pattern of HeLa and Huh7 cells following FUBP3 knockdown, in comparison with control cells. The results showed that FUBP3 knockdown promoted proliferation and inhibited apoptosis of HeLa cells, but inhibited the proliferation of Huh7 cells. FUBP3 knockdown markedly affected the transcriptional level of genes involved in cell adhesion, cell proliferation and the apoptotic process. Furthermore, FUBP3 broadly regulated the alternative splicing of hundreds of genes with functions in cellular component disassembly and the apoptotic process. Validation experiments using reverse transcription-quantitative PCR demonstrated that FUBP3 regulated the expression and alternative splicing of genes associated with cell adhesion, cell proliferation and apoptosis in the HeLa and Huh7 cells lines. These results indicated that FUBP3 could regulate the proliferation and apoptosis of cancer cells perhaps via different gene expression and splicing regulation, which thus furthers the current understanding of the role of FUBP3 in cancer.

Correspondence to: Professor Hongxin Piao, Department of Infectious Diseases, Affiliated Hospital of Yanbian University, 1327 Juzi Street, Yanji, Yanbian Korean Autonomous Prefecture, Jilin 133099, P.R. China
E-mail: 15526770394@163.com

Key words: far upstream element binding protein 3, cell proliferation, apoptosis, RNA-sequencing, gene expression, alternative splicing

Introduction

Cancer has become the leading cause of death in developed countries and the second most common cause of death worldwide (1). Although progress in therapeutic strategies and lifestyle changes (such as reductions in smoking) have resulted in the continuous decline of the cancer mortality rate in recent decades, the incidence of skin melanoma, kidney, pancreatic, liver, mouth and throat cancer continue to rise (2). Furthermore, the poor prognosis of patients with advanced-stage cancer remains an ongoing challenge (3). Thus, it is still necessary to explore the molecular mechanisms mediating occurrence and development of cancer, which is key for early detection and treatment of cancer.

Far upstream element binding protein (FUBP)3 is a member of the FUBP family that comprises three proteins: FUBP1, FUBP2 and FUBP3 (4), which have been found to bind RNA via RNA interactome capture (5). FUBP1 binds to the 3-terminal untranslated region (3' UTR) of the hepatitis C virus RNA to promote viral replication (6). As an RNA binding protein (RBP), FUBP2 promotes the growth and metastasis of cancer cells in non-small cell lung cancer (7). FUBP3 is a RBP and specifically binds to the UG enrichment sequence of the 3' UTR region on fibroblast growth factor 9 (FGF9) mRNA to regulate the expression of FGF9 protein (8). FUBP3 can also bind to the 3' UTR of β-actin mRNA, which is essential for β-actin mRNA localization (9). FUBP1, FUBP2 and FUBP3 belong to a family of single-stranded DNA-binding proteins and possess the general characteristics of conventional transcription factors (4). These proteins primarily participate in transcriptional regulation by recognizing and binding to the far-upstream element (FUSE) on single-stranded DNA. During the early stages of the transcription cycle, the helicase activity of transcription factor IIH promotes the unwinding of

the FUSE, after which FUBP1 binds to it, thereby activating the promoter of the proto-oncogene MYC and driving the transcription process (10). This suggests that members of the FUBP family not only serve a role in promoter-proximal regulation but also participate in the regulation of transcription initiation and elongation of key genes by binding to distant regulatory elements at stages when chromatin structure has not yet fully opened. High expression levels of FBP1 and FBP3 are significantly correlated with c-Myc expression in renal cell carcinoma, supporting their role as potential activators of the c-Myc proto-oncogene in this tumor type (11). Given that FUBPs are DNA- and RNA-binding proteins, they serve a pivotal regulatory role in cancer (12). Upregulation of FUBP1 and FUBP2 can promote cell proliferation and migration in hepatocellular carcinoma cells (13). However, the functions of FUBP1 varies in different types of cancer, reported to act as both an oncogenic protein and a tumor suppressor (12). Notably, FUBP1, a paralog of FUBP3, is a widespread regulator of the alternative splicing of tumor suppressor and oncogene genes (14). FUBP3 was also found to have increased expression levels in hepatocellular carcinoma, which was significantly associated with tumor progression and patient survival rates (15). FUBP3 was shown to regulate chronic myeloid leukemia progression through interactions with the PRC2 complex, which in turn regulates the PAK1-ERK signaling axis (16). Therefore, as an RNA and DNA-binding protein, it can be suggested that FUBP3 influences the occurrence and development of cancer by regulating gene expression and RNA splicing.

The present study hypothesized that FUBP3 serves an important role in cancer cells by broadly regulating gene expression at the transcriptional and post-transcriptional levels. Short hairpin RNA (shRNA) and small interfering RNA (siRNA) for FUBP3 were constructed and transfected into HeLa and Huh7 cells to knockdown FUBP3 expression, following which the effect of FUBP3 knockdown on the proliferation and apoptosis were measured. To investigate the role of FUBP3 in regulating gene expression and alternative splicing, RNA-sequencing (RNA-seq) was performed following FUBP3 knockdown in HeLa cells. The identified changes in gene expression and alternative splicing patterns were further validated in both HeLa and Huh7 cells. The present study aimed to elucidate the regulatory functions of FUBP3 in tumor-associated genes and to explore its context-dependent roles across different cancer cell types, in order to provide functional insights that may inform targeted cancer therapy strategies.

Materials and methods

Cloning and plasmid construction. Sense and antisense strands were annealed to generate the shRNAs. The plasmid vector pGFP-B-RS was digested with *Hind*III and *Bam*HI at 37˚C for 2-3 h. The enzyme-digested vector was run on a 1.0% agarose gel stained with SYBR Safe (1X; Thermo Fisher Scientific, Inc.), visualized under blue light illumination, and purified using a column kit (Qiagen GmbH). The linearized vector DNA, digested with *Hind*III and *Bam*HI, was ligated using T4 DNA Ligase (New England BioLabs, Inc.) to the shRNA insert (5'-GACGGTAATAACGGAAGAATT-3'), which specifically targets the 3'UTR of FUBP3 mRNA. As a negative control, a non-targeting shRNA insert (5'-TTCTCC GAACGTGTCACGT-3') was designed and cloned into the same vector following an identical procedure.

Plasmids were introduced into *Escherichia coli* by chemical transformation. Cells were plated onto LB plates containing kanamycin (50 μg/ml; MilliporeSigma) and incubated overnight at 37˚C. Colonies were screened by colony PCR (30 cycles) using universal primers located on the vector backbone. The forward primer sequence was 5'-GACGTT GTAAAACGACGGCCAG-3' (M13 forward) and the reverse primer sequence was 5'-CAGGAAACAGCTATGACC-3' (M13 reverse). The PCR mixture contained 2X Taq Master Mix (Vazyme Biotech Co., Ltd.). The thermocycling conditions were as follows: Initial denaturation at 95˚C for 3 min; followed by 30 cycles of denaturation at 95˚C for 30 sec, annealing at 55˚C for 30 sec and extension at 72˚C for 30 sec; with a final extension at 72˚C for 5 min. The PCR products were analyzed by electrophoresis on a 1.5% agarose gel stained with SYBR Safe (1X) and visualized under blue light. The interference sequence of shRNA was verified by Sanger sequencing. In addition, three different siRNA (5'-CCAGGA AAGAGACGGCUUUTT-3', 5'-GGCGAUUUCAACUCU CGAATT-3', and 5'-GCAGAUUUCACGGAUUCAATT-3') and non-targeting control siRNA (5'-UUCUCCGAACGU GUCACGUTT-3') were purchased from Suzhou GenePharma Co., Ltd. to knockdown FUBP3.

Cell culture and transfection. The human cervical carcinoma HeLa cell line was obtained from The China Center for Type Culture Collection (cat. no. GDC0009). The Huh7 human hepatocellular carcinoma cell line was purchased from Procell Life Science & Technology Co., Ltd. (cat. no. CL-0120). HeLa and Huh7 cells were cultured at 37˚C with 5% CO_2 in Dulbecco's modified Eagle's medium (DMEM; Gibco; Thermo Fisher Scientific, Inc.) with 10% fetal bovine serum (Shanghai Yeasen Biotechnology Co., Ltd.), 100 μg/ml streptomycin and 100 U/ml penicillin (Gibco; Thermo Fisher Scientific, Inc.). Plasmid transfection of the HeLa or Huh7 cells was performed using Lipofectamine® 2000 (Invitrogen; Thermo Fisher Scientific, Inc.), according to the manufacturer's protocol. Briefly, 1 μg of plasmid DNA was used per well of a 6-well plate. The transfection mixture was incubated with cells at 37˚C for 6 h before replacing the medium. For shRNA knockdown, a non-targeting shRNA vector was transfected into HeLa cells as the negative control. Transfected cells were harvested after 48 h for reverse transcription-quantitative PCR (RT-qPCR) analysis.

Assessment of gene expression. Total RNA was extracted using TRIzol® reagent (Ambion; Thermo Fisher Scientific, Inc.) cDNA synthesis was performed using the Bestar qPCR RT Kit (DBI Bioscience; Shanghai Xinghan Biotechnology Co., Ltd.) according to the manufacturer's protocol. RT-qPCR was then performed on the S1000 Thermal Cycler (Bio-Rad Laboratories, Inc.) using the same Bestar SYBR Green RT-PCR Master Mix (DBI Bioscience). GAPDH was used as a reference gene for assessing the effects of FUBP3 knockdown. Primer sequences are presented in Table SI. The thermocycling conditions for qPCR were as follows: Initial denaturation

at 95˚C for 10 min; followed by 40 cycles of denaturation at 95˚C for 15 sec, and annealing/extension at 60˚C for 1 min. The expression level of each transcript was then normalized to GAPDH mRNA level using the $2^{-\Delta\Delta Cq}$ method (17).

Apoptosis and proliferation analysis. For the analysis of apoptosis, HeLa cells were collected and stained with the Annexin V-PE/7-AAD Apoptosis Detection kit (cat. no. 40304ES60; Shanghai Yeasen Biotechnology Co., Ltd.), according to the manufacturer's protocol. Briefly, 7-AAD cannot penetrate the intact cell membrane of normal and early apoptotic cells; however, in late apoptotic and necrotic cells, 7-AAD can bind to the nucleus through the cell membrane, and thus stained red. Therefore, viable cells are negative for Annexin V-PE and 7-AAD and early apoptotic cells are Annexin V-PE-positive and 7-AAD-negative. Cells positive for both Annexin V-PE and 7-AAD are considered late apoptotic or dead. Apoptotic cells were detected using flow cytometry (MoFlo XDP High-Speed Cell Sorter; Beckman Coulter, Inc.), and the data were analyzed using the FlowJo™ (version 10; BD Biosciences) software.

Cell Counting Kit-8 (CCK-8) assay. The CCK-8 assay (cat. no. HY-K0301; MedChemExpress) was performed in accordance with the manufacturer's instructions. Cells were incubated with CCK-8 reagent for 2 h at 37˚C. Absorbance was measured at a wavelength of 450 nm using an ELISA plate reader (FC; Thermo Fisher Scientific).

Western blot analysis. Cells were lysed using RIPA buffer (50 mM Tris-HCl, pH 7.4, 150 mM NaCl, 1% NP-40, 0.5% sodium deoxycholate and 0.1% SDS), and protease and phosphatase inhibitors (Roche) were added. Protein concentration was determined using the BCA assay (Thermo Fisher Scientific, Inc.). Equal amounts of protein (20 μg per lane) were separated by 10% SDS-polyacrylamide gel electrophoresis and transferred onto a polyvinylidene fluoride membrane (MilliporeSigma). The membrane blocked at room temperature for 1 h in 5% non-fat milk diluted in tris-buffered saline containing 0.1% Tween-20 (TBST), followed by incubation overnight at 4˚C with anti-FUBP3 primary antibody (1:1,000; Proteintech Group, Inc.) and GAPDH as an internal control (1:5,000; Proteintech Group, Inc.). The membrane was washed three times with TBST and incubated at room temperature with an HRP-conjugated Goat Anti-Rabbit IgG (H+L) secondary antibody (cat. no. SA00001-2; 1:5,000; Proteintech Group, Inc.) for 1 h. Protein bands were visualized using enhanced chemiluminescence substrate (Bio-Rad Laboratories, Inc.) and imaged using a ChemiDoc™ imaging system (Bio-Rad Laboratories, Inc.). Density analysis was performed using the ImageJ software (version 1.54f; National Institutes of Health).

RNA extraction. Total RNA was extracted from HeLa cells using TRIzol reagent (Ambion; Thermo Fisher Scientific, Inc.) and further purified by two rounds of phenol-chloroform extraction. Residual genomic DNA was removed by RQ1 DNase (Promega Corporation) treatment. RNA purity and integrity were assessed by A260/A280 ratio measurement using a Smartspec Plus spectrophotometer (Bio-Rad Laboratories, Inc.) and 1.5% agarose gel electrophoresis. For RNA-seq, RNA integrity was additionally confirmed using an Agilent 2100 Bioanalyzer, and only samples with an RNA integrity number ≥8.0 were used for library preparation.

RNA sequencing. The VAHTS mRNA-seq library preparation kit (cat. no. NR601; Vazyme Biotech Co., Ltd.) was used to prepare the RNA-seq library for each sample with 1 μg of total RNA. Polyadenylated mRNA was purified and fragmented, followed by the synthesis of double stranded cDNA. After end repair and A-tailing, the cDNA was ligated to the VAHTS RNA adapter (Vazyme Biotech Co., Ltd.). The purified ligation products (200-500 bp) were digested with a heat-resistant UDG enzyme, amplified, purified, quantified using a Qubit fluorometer, and stored at -80˚C prior to sequencing.

For high-throughput sequencing, the libraries were prepared according to the manufacturer's instructions and subjected to 150-nt paired-end sequencing on the Illumina HiSeq X™ Ten platform (Illumina, Inc.) using the HiSeq X Ten Reagent Kit v2.5 (cat. no. FC-501-2501; Illumina, Inc.). Prior to sequencing, the final libraries were quantified using a Qubit fluorometer and diluted to a loading concentration of 10 pM for cluster generation on the cBot system.

Raw data clean and alignment. The original reads containing >2 N bases were first discarded. The FastX-Toolkit software (version 0.0.13; http://hannonlab.cshl.edu/fastx_toolkit) was then used to clip adapters and low-quality bases from the raw sequencing reads. Short reads of <16 nt were also removed. Clean reads were compared with the GRch38 genome using the Tophat2 software (version 2.1.1) (18), allowing up to 4 mismatches. Uniquely mapped reads were used for gene read counting and fragments per kilobase of transcript per million mapped reads (FPKM) calculations (19).

Differentially expressed gene (DEG) analysis. The R bioconductor package, edgeR (version 3.34) (20) was applied to screen the RNA-sequencing data for DEGs. A false discovery rate (FDR) <0.05 and a fold change >1.5 or <0.67 were used as the cut-off criteria for DEG recognition.

Alternative splicing analysis. Alternative splicing events (ASEs) and regulated ASEs (RASEs) between samples were defined and quantified using the ABLas pipeline (21,22). In brief, the pipeline detects seven types of classical ASEs based on splice junction reads extracted from RNA-seq alignments. ASEs that were present in both the control and experimental groups were retained for subsequent analysis, and RASEs were defined as ASEs showing a statistically significant difference in the percent spliced in index (PSI) values between the two conditions. The algorithmic implementation and source code for ABLas has been described previously (21,22). ABLas detected 10 ASE types based on splice junction reading, including exon skipping (ES), selective 5' splicing site (A5SS), selective 3' splicing site (A3SS), intron-retention (IR), mutually exclusive exons, mutually exclusive 5' UTRs, mutually exclusive 3' UTRs, box exons, A3SS & ES and A5SS & ES. To evaluate the regulatory effects of FUBP3 on ASEs, the significance of changes in the PSI values of each ASE was assessed using a two-tailed β-binomial test. Events with a

P-value <0.05 and a FDR <0.05 were considered significantly FUBP3-regulated ASEs.

RT-qPCR validation of DEGs and AS events. DEGs identified from the RNA-seq data were validated using RT-qPCR. Total RNA from the RNA-seq library preparation was used as the source of cDNA. RNA was reverse transcribed into cDNA using M-MLV Reverse Transcriptase (Vazyme Biotech Co., Ltd.) with the supplied buffer and dNTPs according to the manufacturer's protocol. q PCR was performed with the StepOne™ RealTime PCR System (Thermo Fisher Scientific, Inc.) using SYBR Green (Shanghai Yeasen Biotechnology Co., Ltd.) as the fluorophore. The forward and reverse primer sequences for each target gene are presented in Table SI (5'→3'). GAPDH was used as the reference gene, and its primer sequences are also provided in Table SI. The thermocycling conditions were as follows: Initial denaturation at 95˚C for 10 min; followed by 40 cycles of denaturation at 95˚C for 15 sec, and annealing/extension at 60˚C for 1 min. PCR amplifications were performed in triplicate for each sample. The expression level of each target gene was normalized to GAPDH and quantified using the $2^{-\Delta\Delta Cq}$ method (17).

RT-qPCR was also used for ASE validation. Primer sequences for ASE detection are shown in Table SII. To detect alternative isoforms, a boundary-spanning primer for the sequence encompassing the junction of constitutive exon and alternative exon as well as an opposing primer in a constitutive exon was used. The boundary-spanning primer of alternative exon was designed according to 'model exon' to detect model splicing or 'altered exon' to detect altered splicing. To detect other isomers, a crossover primer sequence, including the junction of the constituent exons and the substituent exons, and an opposite primer in the constituent exons were used. Crossover primers with exons are selected to detect model splicing according to the 'model exon' design or splicing changes are detected according to the 'change exon' design.

Functional enrichment analysis. To evaluate the functional categories of DEGs, Gene Ontology (GO; http://geneontology.org) terms and Kyoto Encyclopedia of Genes and Genomes (KEGG; https://www.kegg.jp) pathways were identified using the KOBAS server (version 2.0; http://kobas.cbi.pku.edu.cn) (23). Hypergeometric test and Benjamini-Hochberg FDR controlling procedure were used to define the enrichment of each term, with a corrected P-value of <0.05 as the significance cut-off.

Statistical analyses. Statistical analyses were performed using GraphPad Prism or R software (version 9.5; GraphPad Software, Inc.) and R software (version 4.2.1; https://www.r-project.org/). For cell proliferation, apoptosis and RT-qPCR data, comparisons between two groups were evaluated using unpaired, two-tailed Student's t-test. For comparisons involving multiple groups, one-way ANOVA was applied followed by Tukey's post hoc test. Multiple testing corrections were applied where indicated. Data are presented as mean ± standard deviation. All experiments were performed with at least three biological replicates, except for RNA-seq, for which key findings were validated by orthogonal methods with increased replicates. P<0.05 was considered to indicate a statistically significant difference.

Results

FUBP3 represses cell proliferation and promotes apoptosis in HeLa cells. In order to determine the effect of FUBP3 on the biological characteristics of HeLa cells, FUBP3 shRNA (shFUBP3) transfection was used to knockdown the expression of FUBP3; RT-qPCR was used to confirm the significant downregulation of FUBP3 in the experimental group, compared with the shNC control cells (Fig. 1A). The repression of FUBP3 significantly promoted cell proliferation (Fig. 1B). Furthermore, three siRNAs were used to knockdown FUBP3 in Huh7 cells; all three showed significant downregulation of FUBP3 compared with siNC control cells (Fig. 1C). The most significantly downregulated siRNA (siFUBP3-3) was used in the subsequent CCK-8 assay. The results of CCK-8 assays showed that shFUBP3 promoted the proliferation of HeLa cells, while siFUBP3 inhibited the proliferation of Huh7 cells (Fig. 1D). Apoptosis levels were evaluated in HeLa cells; apoptosis was inhibited upon FUBP3 knockdown in HeLa cells (Fig. 1E). These results indicate that FUBP3 inhibited cell proliferation and promoted apoptosis in HeLa cells, whereas it promotes cell proliferation in Huh7 cells. A schematic diagram of the mechanism is shown in Fig. S1. Additionally, the transfection results were further validated by western blot (Fig. S2A and B) and the expression levels of FUBP3 were higher in HeLa cells compared with that in Huh7 cells (Fig. S2C).

FUBP3 knockdown affects the gene expression profile of HeLa cells. To explore the genome-wide targets of FUBP3 in HeLa cells, the gene expression profiles shFUBP3 and control cells were determined using RNA-seq; 4 RNA-seq libraries of shFUBP3 and control HeLa cells were constructed and sequenced, with two biological replicates in each group (shCtrl_1st, shCtrl_2nd, shFUBP3_1st and shFUBP3_2nd). Following removal of the sequence adaptors and low-quality reads, an average of 72.1 million clean pair-end reads per sample was obtained; the clean reads were mapped to the human genome, with ~80 percent mapped (Table SIII).

FPKM were used to normalize the mapped reads on each gene and represented gene expression level. The results showed that 22,925 (FPKM >0) and 13,306 genes were expressed at an expression level of FPKM >1 in at least one sample (Tables SIV and SV). RNA-seq demonstrated that FUBP3 was significantly knocked down in the experimental group compared with the control group (Fig. 2A). A correlation matrix was calculated based on the FPKM values of expressed genes in all four samples, which showed that shFUBP3 and control samples were notably separated (Fig. 2B). These findings demonstrated that shFUBP3 affected the gene expression profile of HeLa cells.

In order to further compare the gene expression profiles, the edgeR package was used to identify the DEGs between the shFUBP3 and control cells. There were 599 upregulated and 425 downregulated genes between shFUBP3 and control cells, indicating that shFUBP3 extensively regulates gene expression in HeLa cells (Fig. 2C; Table SVI). Furthermore, hierarchical clustering of normalized FPKM values of DEGs showed a notable separation of the shFUBP3 and control samples, and a high consistency for the two replicate data sets (Fig. 2D).

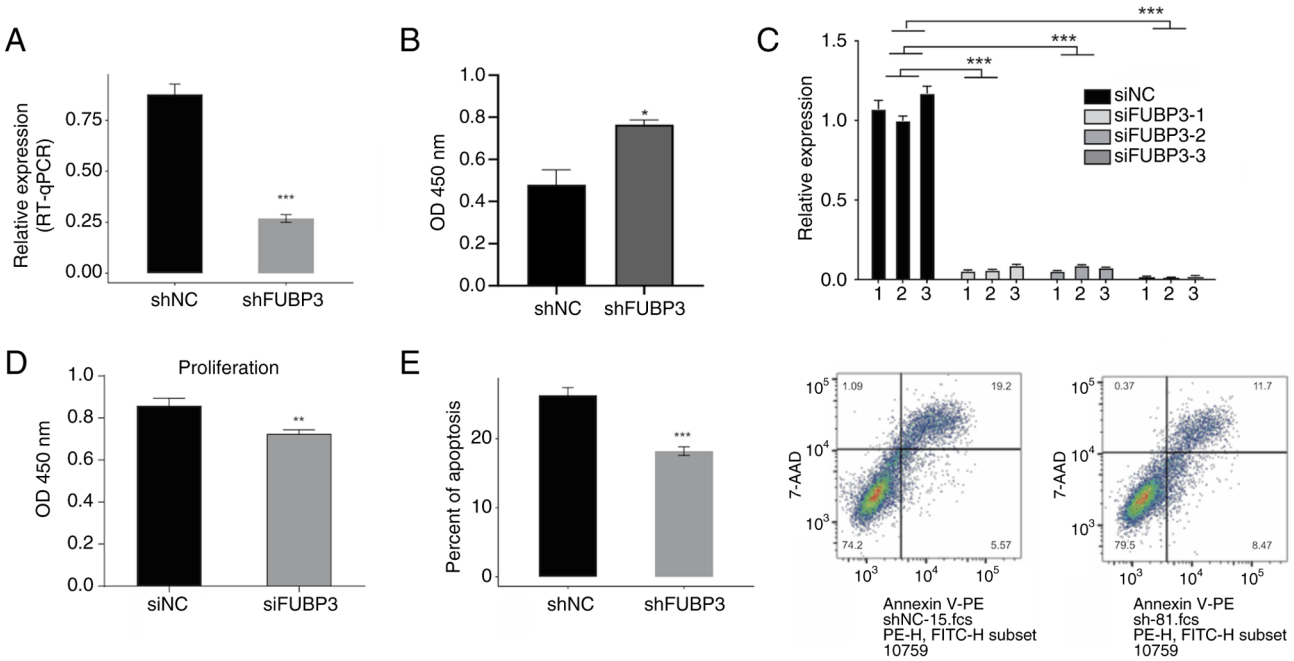

Figure 1. Effect of FUBP3 knockdown on proliferation and apoptosis in HeLa and Huh7 cells. (A) FUBP3 knockdown was verified by RT-qPCR in HeLa cells (n=3). (B) FUBP3 knockdown promotes the proliferation of HeLa cells (n=3). (C) FUBP3 knockdown was verified by RT-qPCR in Huh7 cells (n=3). (D) FUBP3 knockdown represses the proliferation of Huh7 cells (n=8). (E) FUBP3 knockdown represses the apoptosis of HeLa cells (n=4). The flow cytometry gating figure showing the decreased apoptosis level by shFUBP3 (right panel). The gating strategy was as follows: Cells were first gated on FSC/SSC to exclude debris, followed by Annexin V-PE versus 7-AAD gating to distinguish viable, early apoptotic and late apoptotic/dead populations. GAPDH was used as the reference gene for RT-qPCR. Student's t-test was performed to compare FUBP3 knockdown and shNC (for HeLa) or siNC (for Huh7) control cells; P<0.05 was considered to indicate a statistically significant difference. *P<0.05, **P<0.01 and ***P<0.001. FUBP3, far upstream element binding protein 3; RT-qPCR, reverse transcription-quantitative PCR; sh, short hairpin; si, small interfering; shNC, non-targeting shRNA control; siNC, non-targeting siRNA control.

These results indicated that shFUBP3 markedly altered the transcription profile of HeLa cells.

FUBP3 knockdown affects expression of genes involved in cell adhesion, cell proliferation and apoptotic process in HeLa cells. To evaluate the potential roles of DEGs, GO function analysis was performed to annotate all 1,024 DEGs. The results revealed 180 upregulated and 101 downregulated genes annotated with GO categories biological process terms, respectively. The upregulated DEGs were enriched in 65 GO terms and the downregulated DEGs in 26 GO terms (Table SVII). The upregulated genes in shFUBP3 cells that were significantly enriched included the 'collagen catabolic process', 'extracellular matrix disassemble' and 'collagen fibril organization'. The downregulated genes that were significantly enriched included 'negative regulation of inflammatory response', 'positive regulation of cell proliferation' and 'cell adhesion' (Fig. 2E). Notably, both upregulated and downregulated genes were enriched in terms of cell adhesion, cell proliferation and apoptotic process (Table SVII). These findings indicated that shFUBP3 affected the expression of genes involved in cell adhesion, proliferation and apoptosis of HeLa cells.

KEGG pathway analysis was performed to further reveal the functional roles of FUBP3-regulated genes in HeLa cells. The top ten enriched upregulated pathways included 'inflammatory bowel disease', 'rheumatoid arthritis', 'graft-versus-host disease', 'intestinal immune network for IgA production' and 'antigen processing and presentation', all of which were immune and inflammatory associated pathways (Fig. 2F). The top ten enriched downregulated pathways with FUBP3 knockdown included 'ECM-receptor interaction', 'focal adhesion', 'NOD-like receptor signaling pathway', 'Jak-STAT signaling pathway' and 'PI3K-Akt signaling pathway' (Fig. 2F). These findings indicated that FUBP3 affected the expression of genes associated with signal transduction during immune response in cancer.

To verify the effect of shFUBP3 on the expression levels of these DEGs, qPCR was conducted to quantify the changes in mRNA levels of these genes; 10 DEGs with FPKM >1 in at least one sample were selected for qPCR analysis. These DEGs included genes being annotated with cell adhesion (*COL9A2*, *LAMC2*, *PDZD2* and *THBS1*), cell proliferation (*ODC1*, *FBXO2*, *FGFBP1* and *EDN2*) and the apoptotic process (*SNCA* and *BMF*). The RT-qPCR results showed that 8 of 10 selected DEGs showed either a significant increase or decrease in the shFUBP3 HeLa cells compared with that of controls and were consistent with that of the RNA-seq results (Fig. 3). Western blot analysis confirmed the levels of BMF and COL9A2 were consistent with the RT-qPCR results. Taken together, these results indicated that FUBP3 could regulate the expression of genes involved in cell adhesion, cell proliferation and apoptotic processes in HeLa cells.

FUBP3 regulated the alternative splicing of genes associated with apoptosis. FUBP1 is reported to serve a role in regulation of alternative splicing (14). The present study investigated whether FUBP3 also affects RNA splicing in cancer cells. The present RNA-seq data demonstrated the genome-wide splicing targets of FUBP3 identified in HeLa cells. The splice

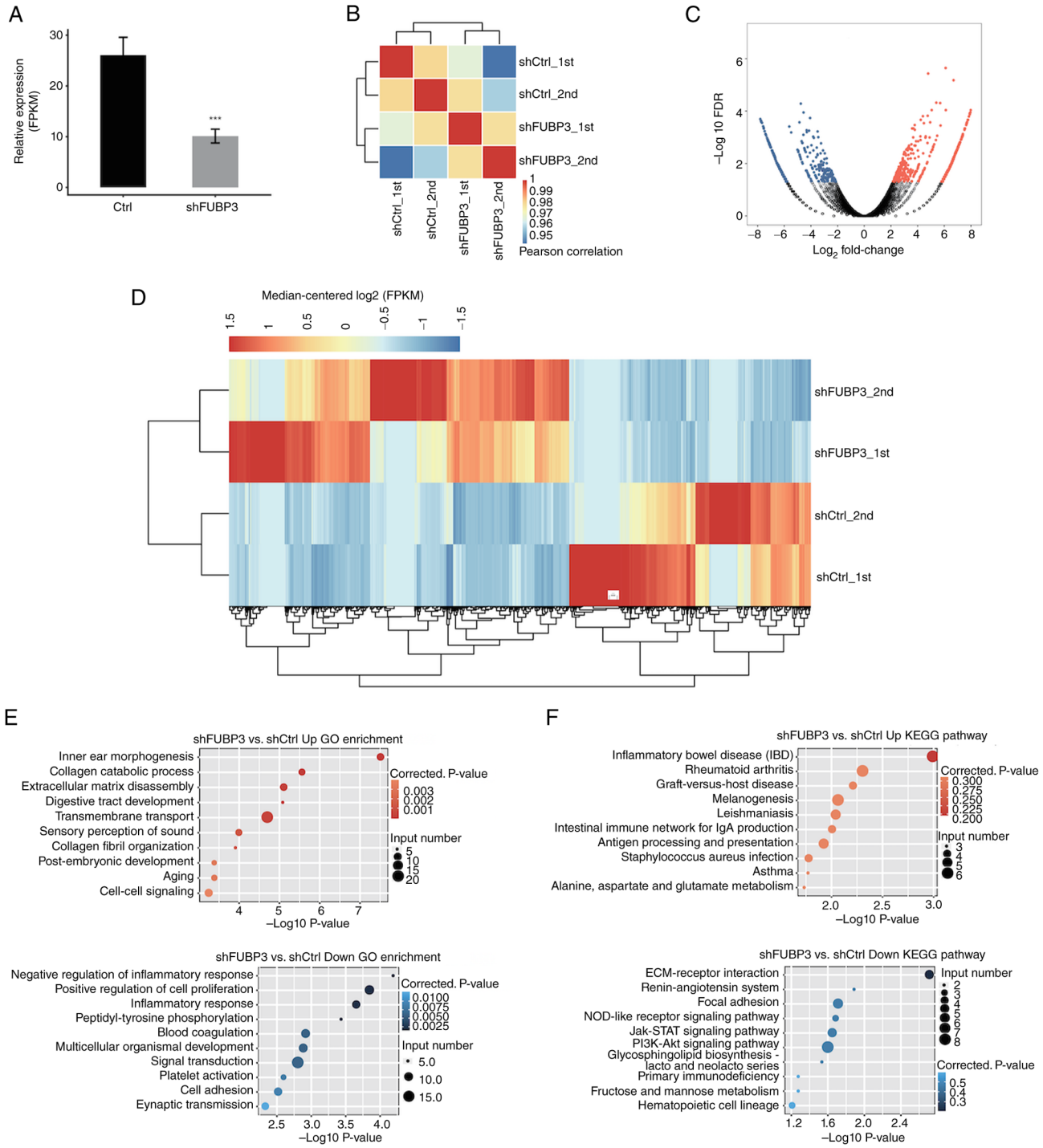

Figure 2. RNA-seq analysis of HeLa cells following shFUBP3 silencing. (A) *FUBP3* gene expression was quantified by RNA-seq. (B) The heat map shows the hierarchically clustered Pearson's correlation matrix resulting from comparing the transcript expression values for shFUBP3 and control samples. (C) Volcano plot of *FUBP3*-regulated genes. Upregulated genes are labelled in red, and downregulated genes are labelled in blue. (D) Hierarchical clustering of the differentially expressed genes between shFUBP3 and control samples. FPKM values are log2-transformed and then median-centered by each gene. (E) The top 10 GO biological processes of *FUBP3*-upregulated and downregulated genes. (F) The top 10 KEGG pathways of *FUBP3*-upregulated and downregulated genes. ***P<0.001. *FUBP3*, far upstream element binding protein 3; RNA-seq, RNA sequencing; sh, short hairpin; GO, Gene Ontology; KEGG, Kyoto Encyclopedia of Genes and Genomes; FPKM, fragments per kilobase of transcript per million mapped reads.

reads from shFUBP3 and control HeLa cells (Table SIII) were mapped to the reference genome, and 219,550 annotated exons (59.77% of total annotated genes) were detected (Table SVIII). Subsequently, the TopHat2 software was used to identify the splice junctions (18). A total of 148,987 known and 85,878 novel splice junctions were identified (Table SVIII). Using the ABLas pipeline, 15,634 known ASEs and 42,259 novel ASEs were detected (Table SIX).

A custom pipeline was performed to identify the FUBP3-RASEs by comparing the changes the ratio of splicing reads between shFUBP3 and control cells, with a cut-off of P-value ≤0.05. A total of 441 RASEs were identified by this

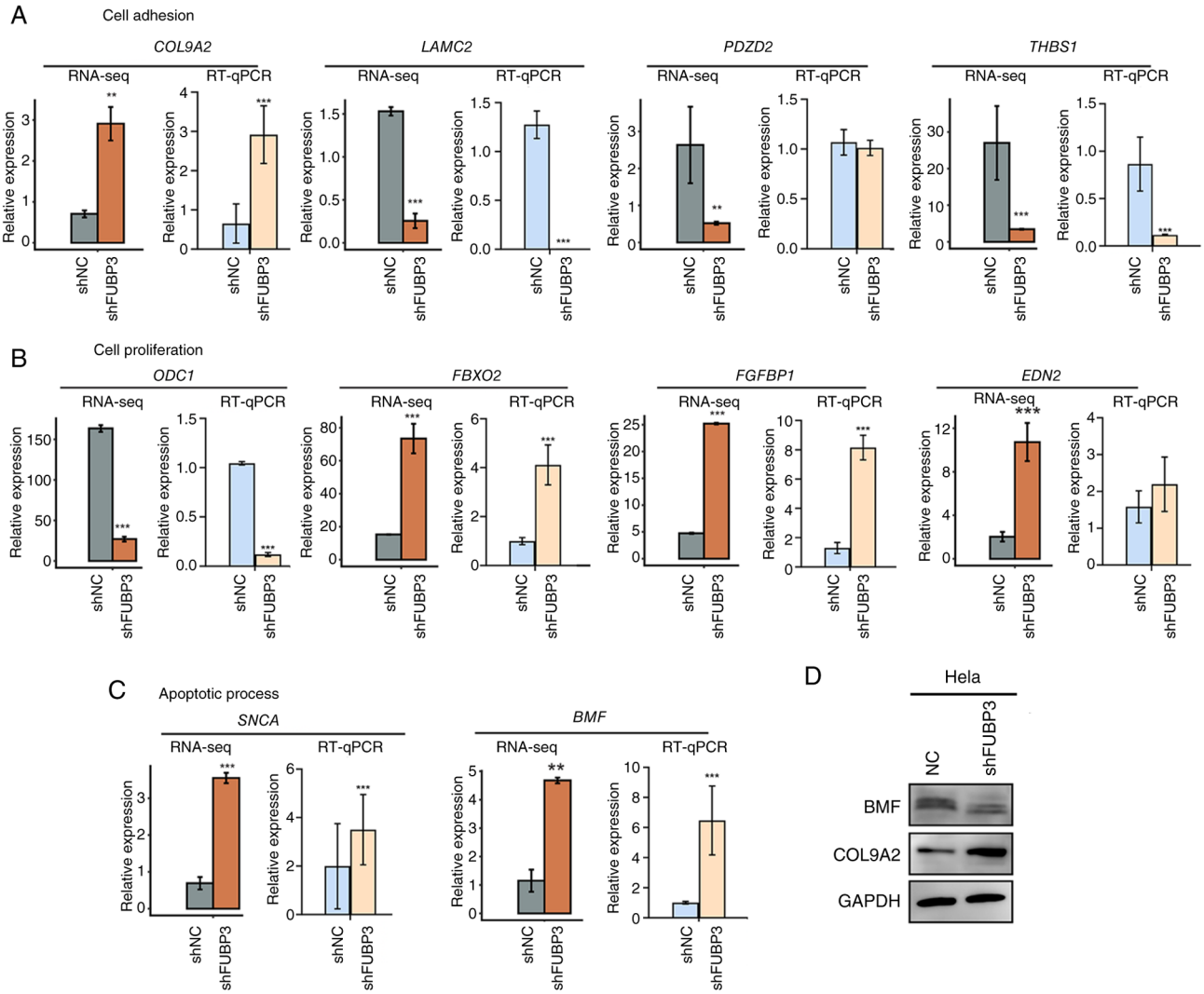

Figure 3. Relative expression levels of selected differentially expressed genes as determined by RNA-seq, RT-qPCR and western blot. Bar plots showing the expression levels of the selected genes associated (A) cell adhesion, (B) cell proliferation and (C) the apoptotic process (n=3). FPKM values of RNA-seq and relative expression by RT-qPCR were present. For RT-qPCR, *GAPDH* was used as the reference gene. (D) Representative western blot experiments. Student's t-test was performed to compare shFUBP3 and shNC control cells; P<0.05 was considered to indicate a statistically significant difference. **P<0.01, ***P<0.001. *FUBP3*, far upstream element binding protein 3; RNA-seq, RNA sequencing; sh, short hairpin; RT-qPCR, reverse transcription-quantitative PCR; FPKM, fragments per kilobase of transcript per million mapped reads; shNC, non-targeting shRNA control; KD, knockdown; *COL9A2*, collagen type IX α2 chain; *LAMC2*, laminin subunit γ2; *PDZD2*, PDZ domain containing 2; *THBS1*, thrombospondin 1; *ODC1*, ornithine decarboxylase 1; *FBXO2*, F-box protein 2; *FGFBP1*, fibroblast growth factor binding protein 1; *EDN2*, endothelin 2; *SNCA*, synuclein α; *BMF*, Bcl-2 modifying factor.

condition, with 138 IR AS events and 303 other types AS events, such as non-IR (NIR) events (Table SIX). A large proportion of the NIR events were A5SS (n=74), A3SS alternative 3'-splice site (n=69) and ES (n=62) (Fig. 4A). Genome location analysis revealed that these FUBP3-regulated ASEs occurred in a total of 406 genes, referred to as regulated alternative splicing genes (RASGs). Overlapping analysis showed that nine genes exhibited changes in both expression levels and alternative splicing pattern (Fig. 4B).

To explore the potential function of RASGs, GO term analysis was conducted. GO biological process annotation showed that RASGs were enriched in 'cellular component disassembly' and 'apoptotic process' (Fig. 4C). KEGG biological process annotation showed that RASGs were enriched in 'pyrimidine metabolism' and 'metabolic pathways' (Fig. 4D).

qPCR was used to validate the effects of FUBP3 on alternative splicing of five genes. The changes in ratio of the five detected RASEs via qPCR were in agreement with that of transcriptome analysis (Fig. 4E-G). Notably, a cassette Exon event occurred at *NUP62* gene after FUBP3 knockdown in HeLa cells (Fig. 4E). The *CDK2* showed an exon skipping event after FUBP3 knockdown (Fig. 4F). *CTNND1* was spliced at A3SS and *GSN* was spliced at A5SS after FUBP3 knockdown in HeLa cells (Fig. 4G).

Validation of FUBP3 regulated gene expression and alternative splicing in a liver cancer cell line. In order to verify the regulation role of FUBP3 in other cell lines, parallel validation experiments were performed in the Huh7 liver cancer cell line. The expression levels of FUBP3 were assessed in the shFUBP3 and siNC Huh7 cells via RT-qPCR. Regarding the aforementioned DEGs identified, the expression of the ten genes were validated using RT-qPCR. FUBP3 could regulate the expression of these genes in the liver cancer cells, and the expression

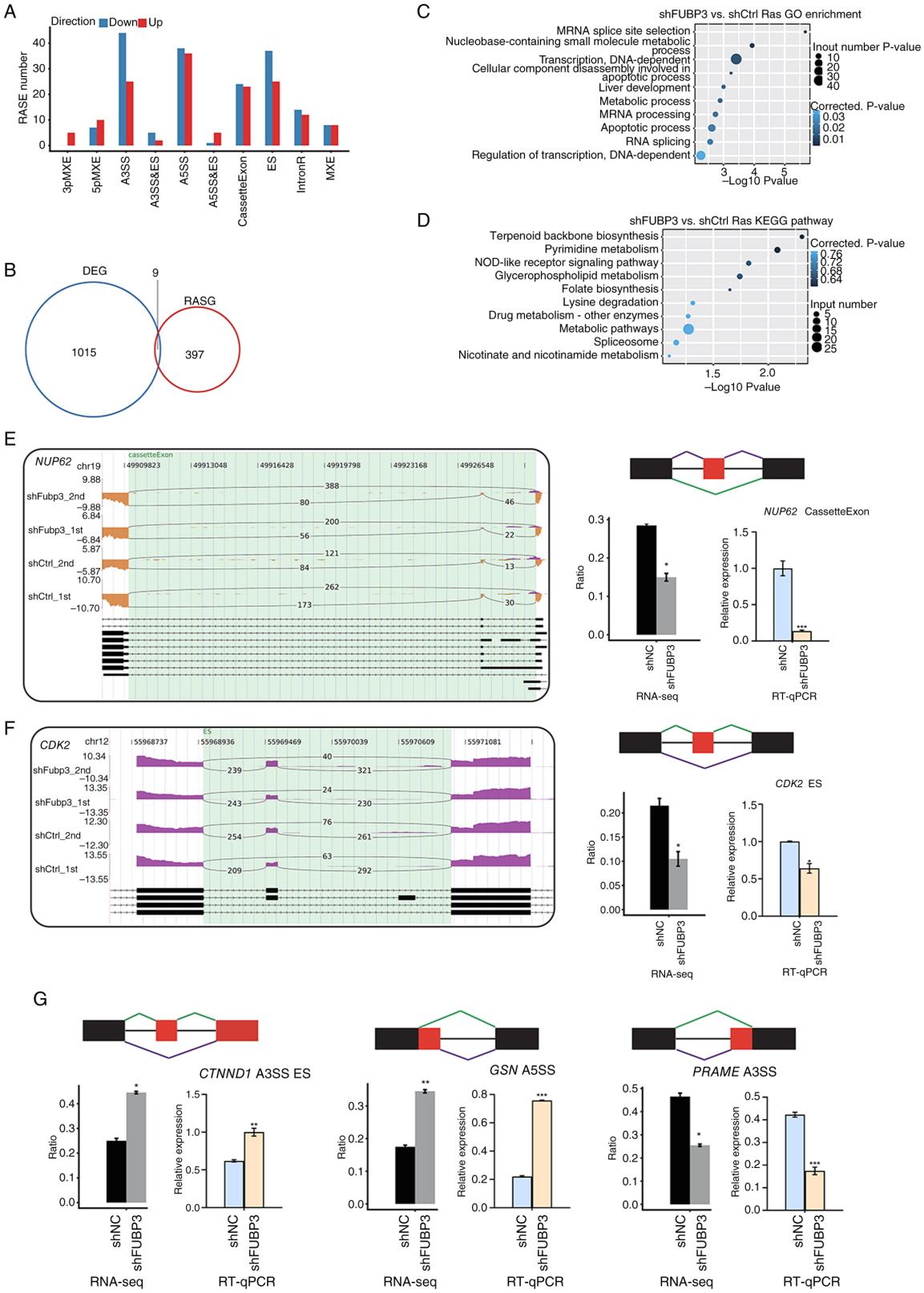

Figure 4. Identification and functional analysis of FUBP3-regulated splicing events and genes. (A) Classification of different AS types regulated by FUBP3 protein. (B) The overlap analysis between FUBP3-regulated DEG and FUBP3-RASGs. (C) The top 10 GO biological process analyses. (D) The top 10 KEGG biological processes. (E-G) Validation of FUBP3-RASEs. For each panel, the left panel shows AIGV-sashimi plots of AS changes in shFUBP3 and shNC cells, with gene transcript structures shown below. The right panel (top) shows schematic diagrams of the AS events, AS1 (purple line) and AS2 (green line). The right panel (bottom) shows RNA-seq quantification and RT-qPCR validation. The altered ratio of AS events was calculated as: AS1 junction reads/(AS1 junction reads + AS2 junction reads) for RNA-seq, and AS1 transcript level/AS2 transcript level for RT-qPCR. n=2 for RNA-seq; n=3 for RT-qPCR. Student's t-test was performed to compare shFUBP3 and shNC cells; *P<0.05, **P<0.01 and ***P<0.001. (E) Validation at the *NUP62* gene. (F) Validation at the *CDK2* gene. (G) Validation at the *CTNND1*, *GSN* and *PRAME* genes. *CTNND1* shows an A3SS/ES event, *GSN* shows an A5SS event and *PRAME* shows an A3SS event. *FUBP3*, far upstream element binding protein 3; RNA-seq, RNA sequencing; sh, short hairpin; KD, knockdown; GO, Gene Ontology; KEGG, Kyoto Encyclopedia of Genes and Genomes; FPKM, fragments per kilobase of transcript per million mapped reads. AS, alternative splicing; RASGs, regulated AS genes; RT-qPCR, reverse transcription-quantitative PCR; ES, exon skipping; A5SS, selective 5' splicing site; A3SS, selective 3' splicing site.

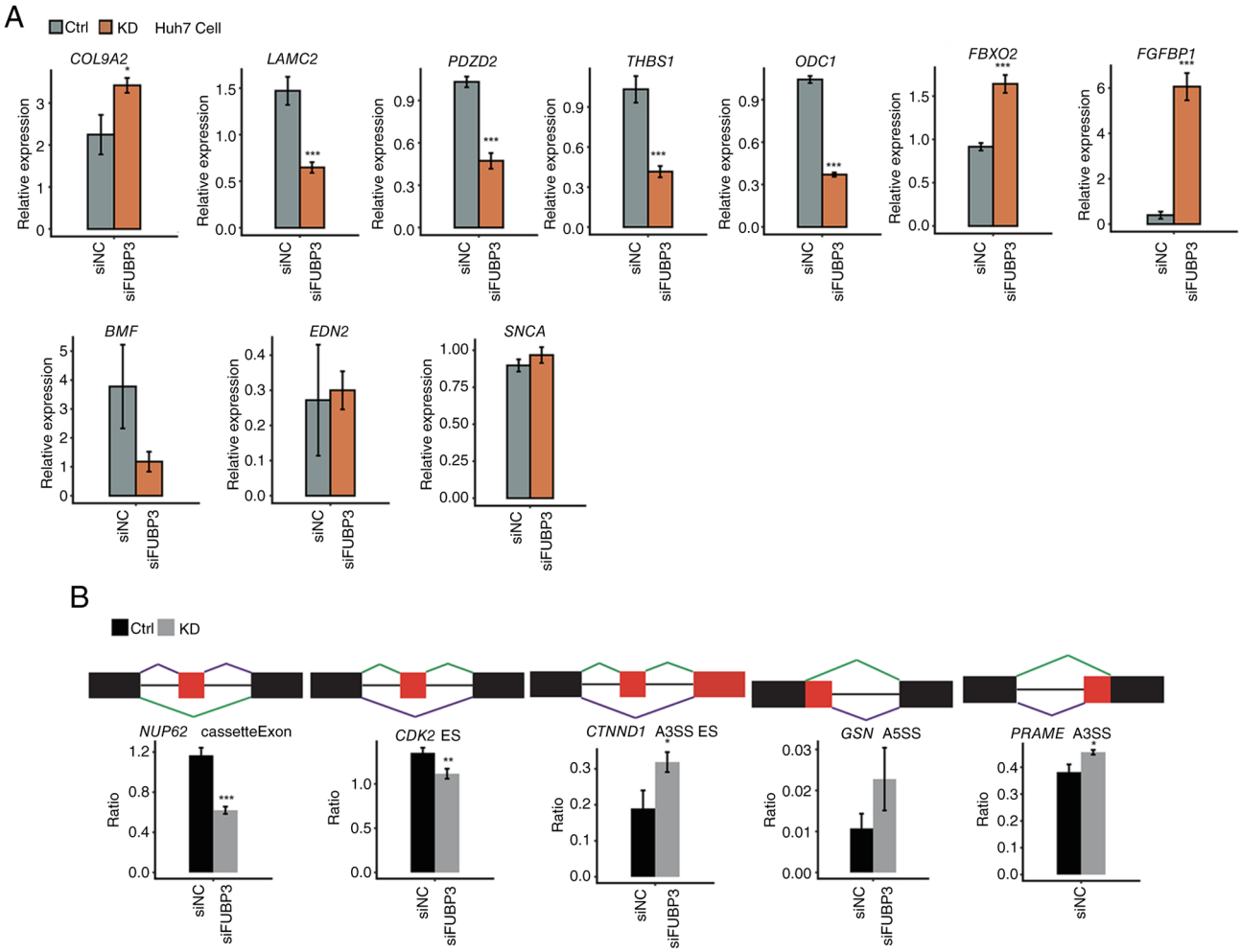

Figure 5. Validation of FUBP3-regulated gene expression and ASEs in Huh7 cells. (A) Relative expression levels of selected genes measured by RT-qPCR in siFUBP3 and siNC Huh7 cells. For RT-qPCR, *GAPDH* was used as the reference gene (n=3). (B) Validation of FUBP3-RASEs in Huh7 cells. The schematic diagrams depict the structures of ASEs, AS1 (purple line) and AS2 (green line). The exon sequences are denoted by boxes and intron sequences by the horizontal line (top), and RT-qPCR validation of ASEs (bottom). The altered ratio of AS events in qPCR was calculated using the formula: AS1 transcripts level/AS2 transcripts level (n=3). Student's t-test was performed to compare siFUBP3 and control cells; $P<0.05$ was considered to indicate a statistically significant difference. $^{*}P<0.05$, $^{**}P<0.01$ and $^{***}P<0.001$. ASE, alternative splicing events; RASE, regulated ASE; *FUBP3*, far upstream element binding protein 3; RNA-seq, RNA sequencing; sh, short hairpin; KD, knockdown; RT-qPCR, reverse transcription-quantitative PCR; *COL9A2*, collagen type IX α2 chain; *LAMC2*, laminin subunit γ2; *PDZD2*, PDZ domain containing 2; *THBS1*, thrombospondin 1; *ODC1*, ornithine decarboxylase 1; *FBXO2*, F-box protein 2; *FGFBP1*, fibroblast growth factor binding protein 1; *EDN2*, endothelin 2; *SNCA*, synuclein α; *BMF*, Bcl-2 modifying factor; ES, exon skipping; A5SS, selective 5' splicing site; A3SS, selective 3' splicing site.

of nine of these genes were in accordance with that found in HeLa cells (Fig. 5A); the expression levels of *BMF* were inconsistent with the results in HeLa cells. Regarding the alternative splicing analysis, the five aforementioned ASEs (Fig. 5B) were validated. The results of the four types of alternative splicing assessed showed that FUBP3 regulates alternative splicing in Huh7 cells, consistent with the observations in HeLa cells. These findings demonstrated that FUBP3 served a role in regulating the expression of genes and alternative splicing in the Huh7 liver cancer cell line.

Discussion

The present study found that FUBP3 knockdown exerts opposite effects on cell proliferation in HeLa cells (promoting apoptosis) and Huh7 cells (promoting proliferation). While this finding is striking, it is not unprecedented, as many RNA-binding proteins exhibit cell-type-specific or context-dependent functions. Several non-mutually exclusive mechanisms may explain this discrepancy. First, there is a significant difference in the basal expression levels of FUBP3 between these two cell lines. The present data indicate that endogenous FUBP3 protein levels in Huh7 cells are approximately half those in HeLa cells. Consequently, knocking down FUBP3 in HeLa cells may reduce its levels below the critical threshold required to maintain certain survival pathways; whereas in Huh7 cells, which already have lower FUBP3 expression levels, further depletion may activate different regulatory networks. Second, the downstream target network of FUBP3 likely exhibits cell-type specificity. FUBP3 regulates transcription and alternative splicing by binding to DNA and RNA; the sets of genes and splicing events affected by FUBP3 knockdown may show significant overlap between HeLa and Huh7 cells, but may also diverge due to differences in chromatin accessibility, the expression of transcription factor partners or the abundance of competing RNA-binding proteins as has been reported for other RNA-binding proteins (5,12).

Third, FUBP3 regulates key splicing factors or apoptosis-related genes (such as BMF and BCL2L11), as suggested by the present RNA-seq data and consistent with reports that FUBP1 regulates alternative splicing (14) in a context-dependent manner. Inconsistent validation results for BMF expression in HeLa cells suggest that FUBP3 may regulate BMF at the splicing rather than the transcriptional level, and that such regulatory mechanisms may be cell type-specific. Fourth, there are differences in the cellular origins and genetic backgrounds of the two cell lines, HeLa cells are derived from cervical adenocarcinoma, while Huh7 cells are derived from hepatocellular carcinoma. These two types of cancer harbor different driver mutations (such as p53 status and alterations in the Wnt/β-catenin pathway) (24), which may interact epigenetically with the outcomes of FUBP3 knockdown. In summary, these two diametrically opposed proliferative effects reflect the complex and context-dependent nature of the FUBP3 regulatory network, rather than a simple 'on-off' switch. Elucidating the precise molecular determinants of this cell-type specificity, for example, by comparing the FUBP3 interaction networks or chromatin binding profiles across the two cell lines, represents an important direction for future research (15).

A previous study reported that upregulation of FUBP3 is associated with tumor progression and poor survival in hepatocellular carcinoma (15), suggesting that FUBP3 may act as an oncogene in this cancer type. In the present study, knockdown of FUBP3 promoted the proliferation and inhibited apoptosis of HeLa cells, indicating that FUBP3 served an oncogenic role in HeLa cells. By contrast, knockdown of FUBP3 inhibited the proliferation of Huh7 cells, which also indicated FUBP3 may possess anti-oncogenic properties. Both FUBP3 and FUBP1 are members of the far upstream element binding proteins family (4). FUBP1 functions as an oncogene or anti-oncogene in different types of cells (6,11,12). The present results suggested that FUBP3 could serve different functions in different types of cancer cells, similar to FUBP1. Thus, further investigations, including more robust experimental assays and additional cellular proliferation experiments, should be conducted to further confirm the cellular functions of FUBP3 in other types of cancer.

FUBP3 is a DNA binding transcriptional activator that regulates the expression of certain genes (4). In the present study, the expression levels of 1,024 genes were significantly changed at the transcription level following FUBP3 knockdown in HeLa cells. Functional analysis showed that these genes were important in tumor progression via cell adhesion, cell proliferation and apoptotic process. For example, LAMC2 was upregulated in various types of cancer, which may be a general feature of tumor cell migration (25,26). In breast cancer, THBS1 was regulated by the Hippo component YAP which promotes focal adhesion and tumor aggressiveness (27). In the present study, FUBP3 knockdown decreased the expression of LAMC2 and THBS1, which indicated that FUBP3 may also serve a role in the metastasis of cancer. In addition, FGFBP1 is beneficial to proliferation and differentiation during embryonic development and wound healing (28). FGFBP1 expression is significantly increased in colon and pancreatic cancer compared with low expression in normal adult tissues (29,30), and the upregulation of FGFBP1 also promotes tumor growth and metastasis (31). The promoter region of FGFBP1 has been shown to be directly bound by c-Myc (32); FUBP3 has been reported as a potential regulator of c-Myc in renal cancer, but not in prostate and bladder cancer (11). As a transcription factor and oncoprotein, c-Myc is reported as a potent driver of several types of human cancer and can regulate numerous biological activities that contribute to tumorigenesis (33). It could be hypothesized that FUBP3 regulates FGFBP1 via c-Myc, with FUBP3 acting as a relative upstream signaling regulator. However, FUBP3 knockdown could inhibit the expression of FGFBP1 in HeLa and Huh7 cells. Furthermore, it could not be ascertained whether FUBP3 regulates gene expression directly or indirectly from the present RNA-seq data; thus, it is necessary to further investigate how FUBP3 regulates the expression of these genes.

In previous studies, FUBP3 were reported to bind to RNAs (5,8), demonstrating a role in post-transcriptional regulation. In the present study, alternative splicing patterns of 406 genes were significantly altered after FUBP3 knockdown in HeLa cells. These genes were enriched in pathways including the apoptotic process, DNA repair and the mitosis cycle. Notably, validation experiments showed that FUBP3 could regulate the alternative splicing of *GSN*, *NUP62*, *CDK2* and *CTNND1* in HeLa and Huh7 cells. The *GSN* gene, which encodes for gelsolin, an actin-binding protein that serves a role in PI3K/AKT/mTOR pathway, was detected as one of the most abundant ASEs (present in 34% of head and neck squamous cell carcinoma samples) in a previous study (34,35). Additionally, downregulation of GSN has been shown to downregulate apoptosis, a hallmark of cancer cells (36,37). In previous studies, mechanistically, both miR-298 overexpression and CTNND1 knockdown inhibited Wnt/β-catenin signaling and resulted in reduced expression of β-catenin, WNT11, Cyclin D1 and MMP7 in HCCLM3 cells (a hepatocellular carcinoma cell line) (38). These previous studies showed that the CDK2 target protein, FOXO1, serves a vital part in triggering DNA-damage-induced apoptosis following double strand DNA breaks (31). CDK2 also protects against apoptosis through phosphorylation of the pro-survival factor myeloid leukemia cell differentiation protein (39,40), which is consistent with the present study. Thus, it could be considered that FUBP3 may regulate apoptosis via CDK2. The regulatory effect of FUBP3 on tumor-related genes was revealed, and FUBP3 may have different regulatory functions in different cancer cells. Thus, it is necessary to further investigate how FUBP3 regulates the splicing of these genes.

In summary, FUBP3 regulated the expression and alternative splicing of genes associated with the proliferation and apoptosis of cancer cells. Regulatory effects of FUBP3 on tumor-related genes were also identified, suggesting that FUBP3 may exert different regulatory functions in different types of cancer cells. Based on these findings and the unresolved question of whether FUBP3 regulates its target genes directly or indirectly, the present results provide a basis for the investigation of FUBP3-targeted therapies in cancer, and further studies are warranted to explore the underlying molecular mechanisms of FUBP3.

Acknowledgements

Not applicable.

Funding

This study was supported by the National Natural Science Foundation of China (grant no. 82260506), the National Science and Technology Major Special Project for Infectious Diseases (grant no. 2017ZX10203202003) and the Science and Technology Department of Jilin Province (grant no. YDZJ202201ZYTS233).

Availability of data and materials

The data generated in the present study may be found in the NCBI BioProject database under accession number PRJNA1452872 or at the following URL: https://www.ncbi.nlm.nih.gov/bioproject/PRJNA1452872.

Authors' contributions

LK performed the experiments and and analyzed the data. CF, XL, MC, MZ, TW and XL analyzed, interpreted and validated the data. HP conceived and supervised the study, and revised and wrote the manuscript. HP and LK confirm the authenticity of all the raw data. All authors read and approved the final manuscript.

Ethics approval and consent to participate

Not applicable.

Patient consent for publication

Not applicable.

Competing interests

The authors declare that they have no competing interests.

References

1. Dagenais GR, Leong DP, Rangarajan S, Lanas F, Lopez-Jaramillo P, Gupta R, Diaz R, Avezum A, Oliveira GBF, Wielgosz A, *et al*: Variations in common diseases, hospital admissions, and deaths in middle-aged adults in 21 countries from five continents (PURE): A prospective cohort study. Lancet 395: 785-794, 2020.
2. Siegel RL, Miller KD and Jemal A: Cancer statistics, 2020. CA Cancer J Clin 70: 7-30, 2020.
3. Yao HP, Hudson R and Wang MH: Progress and challenge in development of biotherapeutics targeting MET receptor for treatment of advanced cancer. Biochim Biophys Acta Rev Cancer 1874: 188425, 2020.
4. Davis-Smyth T, Duncan RC, Zheng T, Michelotti G and Levens D: The far upstream element-binding proteins comprise an ancient family of single-strand DNA-binding transactivators. J Biol Chem 271: 31679-31687, 1996.
5. Castello A, Fischer B, Eichelbaum K, Horos R, Beckmann BM, Strein C, Davey NE, Humphreys DT, Preiss T, Steinmetz LM, *et al*: Insights into RNA biology from an atlas of mammalian mRNA-binding proteins. Cell 149: 1393-1406, 2012.
6. Zhang Z, Harris D and Pandey VN: The FUSE binding protein is a cellular factor required for efficient replication of hepatitis C virus. J Virol 82: 5761-5773, 2008.
7. Yan M, Sun L, Li J, Yu H, Lin H, Yu T, Zhao F, Zhu M, Liu L, Geng Q, *et al*: RNA-binding protein KHSRP promotes tumor growth and metastasis in non-small cell lung cancer. J Exp Clin Cancer Res 38: 478, 2019.
8. Gau BH, Chen TM, Shih YH and Sun HS: FUBP3 interacts with FGF9 3' microsatellite and positively regulates FGF9 translation. Nucleic Acids Res 39: 3582-3593, 2011.
9. Mukherjee J, Hermesh O, Eliscovich C, Nalpas N, Franz-Wachtel M, Maček B and Jansen RP: β-Actin mRNA interactome mapping by proximity biotinylation. Proc Natl Acad Sci USA 116: 12863-12872, 2019.
10. Zhou W, Chung YJ, Parrilla Castellar ER, Zheng Y, Chung HJ, Bandle R, Liu J, Tessarollo L, Batchelor E, Aplan PD and Levens D: Far upstream element binding protein serves a crucial role in embryonic development, hematopoiesis, and stabilizing Myc expression levels. Am J Pathol 186: 701-715, 2016.
11. Weber A, Kristiansen I, Johannsen M, Oelrich B, Scholmann K, Gunia S, May M, Meyer HA, Behnke S, Moch H and Kristiansen G: The FUSE binding proteins FBP1 and FBP3 are potential c-myc regulators in renal, but not in prostate and bladder cancer. BMC Cancer 8: 369, 2008.
12. Debaize L and Troadec MB: The master regulator FUBP1: Its emerging role in normal cell function and malignant development. Cell Mol Life Sci 76: 259-281, 2019.
13. Malz M, Weber A, Singer S, Riehmer V, Bissinger M, Riener MO, Longerich T, Soll C, Vogel A, Angel P, *et al*: Overexpression of far upstream element binding proteins: A mechanism regulating proliferation and migration in liver cancer cells. Hepatology 50: 1130-1139, 2009.
14. Elman JS, Ni TK, Mengwasser KE, Jin D, Wronski A, Elledge SJ and Kuperwasser C: Identification of FUBP1 as a long tail cancer driver and widespread regulator of tumor suppressor and oncogene alternative splicing. Cell Rep 28: 3435-3449.e5, 2019.
15. Brauckhoff A, Malz M, Tschaharganeh D, Malek N, Weber A, Riener MO, Soll C, Samarin J, Bissinger M, Schmidt J, *et al*: Nuclear expression of the ubiquitin ligase seven in absentia homolog (SIAH)-1 induces proliferation and migration of liver cancer cells. J Hepatol 55: 1049-1057, 2011.
16. Sharma M, Anandram S, Ross C and Srivastava S: FUBP3 regulates chronic myeloid leukaemia progression through PRC2 complex regulated PAK1-ERK signalling. J Cell Mol Med 27: 15-29, 2023.
17. Livak KJ and Schmittgen TD: Analysis of relative gene expression data using real-time quantitative PCR and the 2(-Delta Delta C(T)) method. Methods 25: 402-408, 2001.
18. Kim D, Pertea G, Trapnell C, Pimentel H, Kelley R and Salzberg SL: TopHat2: accurate alignment of transcriptomes in the presence of insertions, deletions and gene fusions. Genome Biol 14: R36, 2013.
19. Trapnell C, Williams BA, Pertea G, Mortazavi A, Kwan G, van Baren MJ, Salzberg SL, Wold BJ and Pachter L: Transcript assembly and quantification by RNA-Seq reveals unannotated transcripts and isoform switching during cell differentiation. Nat Biotechnol 28: 511-515, 2010.
20. Robinson MD, McCarthy DJ and Smyth GK: edgeR: A Bioconductor package for differential expression analysis of digital gene expression data. Bioinformatics 26: 139-140, 2010.
21. Jin L, Li G, Yu D, Huang W, Cheng C, Liao S, Wu Q and Zhang Y: Transcriptome analysis reveals the complexity of alternative splicing regulation in the fungus Verticillium dahliae. BMC Genomics 18: 130, 2017.
22. Xia H, Chen D, Wu Q, Wu G, Zhou Y, Zhang Y and Zhang L: CELF1 preferentially binds to exon-intron boundary and regulates alternative splicing in HeLa cells. Biochim Biophys Acta Gene Regul Mech 1860: 911-921, 2017.
23. Xie C, Mao X, Huang J, Ding Y, Wu J, Dong S, Kong L, Gao G, Li CY and Wei L: KOBAS 2.0: A web server for annotation and identification of enriched pathways and diseases. Nucleic Acids Res 39 (Web Server Issue): W316-W322, 2011.
24. Landry JJ, Pyl PT, Rausch T, Zichner T, Tekkedil MM, Stütz AM, Jauch A, Aiyar RS, Pau G, Delhomme N, *et al*: The genomic and transcriptomic landscape of a HeLa cell line. G3 (Bethesda) 3: 1213-1224, 2013.
25. Hamasaki H, Koga K, Aoki M, Hamasaki M, Koshikawa N, Seiki M, Iwasaki H, Nakayama J and Nabeshima K: Expression of laminin 5-γ2 chain in cutaneous squamous cell carcinoma and its role in tumour invasion. Br J Cancer 105: 824-832, 2011.
26. Shou JZ, Hu N, Takikita M, Roth MJ, Johnson LL, Giffen C, Wang QH, Wang C, Wang Y, Su H, *et al*: Overexpression of CDC25B and LAMC2 mRNA and protein in esophageal squamous cell carcinomas and premalignant lesions in subjects from a high-risk population in China. Cancer Epidemiol Biomarkers Prev 17: 1424-1435, 2008.

27. Shen J, Cao B, Wang Y, Ma C, Zeng Z, Liu L, Li X, Tao D, Gong J and Xie D: Hippo component YAP promotes focal adhesion and tumour aggressiveness via transcriptionally activating THBS1/FAK signalling in breast cancer. J Exp Clin Cancer Res 37: 175, 2018.
28. Schmidt MO, Garman KA, Lee YG, Zuo C, Beck PJ, Tan M, Aguilar-Pimentel JA, Ollert M, Schmidt-Weber C, Fuchs H, *et al*: The role of fibroblast growth factor-binding protein 1 in skin carcinogenesis and inflammation. J Invest Dermatol 138: 179-188, 2018.
29. Schulze D, Plohmann P, Höbel S and Aigner A: Anti-tumor effects of fibroblast growth factor-binding protein (FGF-BP) knockdown in colon carcinoma. Mol Cancer 10: 144, 2011.
30. Tassi E, Henke RT, Bowden ET, Swift MR, Kodack DP, Kuo AH, Maitra A and Wellstein A: Expression of a fibroblast growth factor-binding protein during the development of adenocarcinoma of the pancreas and colon. Cancer Res 66: 1191-1198, 2006.
31. Huang W, Chen Z, Shang X, Tian D, Wang D, Wu K, Fan D and Xia L: Sox12, a direct target of FoxQ1, promotes hepatocellular carcinoma metastasis through up-regulating Twist1 and FGFBP1. Hepatology 61: 1920-1933, 2015.
32. Harris VK, Coticchia CM, List HJ, Wellstein A and Riegel AT: Mitogen-induced expression of the fibroblast growth factor-binding protein is transcriptionally repressed through a non-canonical E-box element. J Biol Chem 275: 28539-28548, 2000.
33. Lourenco C, Resetca D, Redel C, Lin P, MacDonald AS, Ciaccio R, Kenney TMG, Wei Y, Andrews DW, Sunnerhagen M, *et al*: MYC protein interactors in gene transcription and cancer. Nat Rev Cancer 21: 579-591, 2021.
34. Guo T, Gaykalova DA, Considine M, Wheelan S, Pallavajjala A, Bishop JA, Westra WH, Ideker T, Koch WM, Khan Z, *et al*: Characterization of functionally active gene fusions in human papillomavirus related oropharyngeal squamous cell carcinoma. Int J Cancer 139: 373-382, 2016.
35. Guo T, Sakai A, Afsari B, Considine M, Danilova L, Favorov AV, Yegnasubramanian S, Kelley DZ, Flam E, Ha PK, *et al*: A novel functional splice variant of AKT3 defined by analysis of alternative splice expression in HPV-positive oropharyngeal cancers. Cancer Res 77: 5248-5258, 2017.
36. Fujita H, Laham LE, Janmey PA, Kwiatkowski DJ, Stossel TP, Banno Y, Nozawa Y, Müllauer L, Ishizaki A and Kuzumaki N: Functions of [His321]gelsolin isolated from a flat revertant of ras-transformed cells. Eur J Biochem 229: 615-620, 1995.
37. Winston JS, Asch HL, Zhang PJ, Edge SB, Hyland A and Asch BB: Downregulation of gelsolin correlates with the progression to breast carcinoma. Breast Cancer Res Treat 65: 11-21, 2001.
38. Cao N, Mu L, Yang W, Liu L, Liang L and Zhang H: RETRACTED: MicroRNA-298 represses hepatocellular carcinoma progression by inhibiting CTNND1-mediated Wnt/β-catenin signaling. Biomed Pharmacother 106: 483-490, 2018.
39. Choudhary GS, Al-Harbi S, Mazumder S, Hill BT, Smith MR, Bodo J, Hsi ED and Almasan A: MCL-1 and BCL-xL-dependent resistance to the BCL-2 inhibitor ABT-199 can be overcome by preventing PI3K/AKT/mTOR activation in lymphoid malignancies. Cell Death Dis 6: e1593, 2015.
40. Choudhary GS, Tat TT, Misra S, Hill BT, Smith MR, Almasan A and Mazumder S: Cyclin E/Cdk2-dependent phosphorylation of Mcl-1 determines its stability and cellular sensitivity to BH3 mimetics. Oncotarget 6: 16912-16925, 2015.